Journal of the Oceanographical Society of Japan
Vol. 40, pp. 1 to 11, 1984

Nonlinear Properties of Laboratory Wind Waves at Energy Containing Frequencies

Part 1. Probability Density Distribution of Surface Elevation*

Mitsuhiko Hatori†

Abstract: Nonlinear properties of wind waves in a wind-wave tunnel are investigated by measuring the probability density distribution of surface elevation. The surface elevation distribution of raw records are found to have a positive skewness (K_3=0.21 to 0.43) and a negative kurtosis (K_4=−0.74 to −0.41) with magnitude depending of fetch and wind speed. The values of skewness are in qualitative agreement with a prediction of the weak interaction theory for a random wave field incorporating the effects of second harmonics (Tayfun, 1980), but the values of kurtosis are different in sign from the prediction.

To examine the nonlinear properties of energy containing components, higher harmonic components are excluded from the wave records by using a kind of a band-pass filter. The surface elevation distributions of the filtered waves show a sharp decrease in skewness ($\overline{K_3}'$=0), but the distributions remain highly non-Gaussian with a large negative kurtosis almost independent of the fetch and wind speed ($\overline{K_4}'$=−0.66). It is concluded that the negative kurtosis is due to the non-random character of the phase and amplitude among the energy containing components, and that nonlinear interactions occur amongst the energy containing frequencies.

1. Introduction

Wind waves have long been regarded as a sum of linear irrotational waves with random phases to a first order approximation. Higher order nonlinear corrections to such a random wave field were first made by Tick (1959), Phillips (1960), Hasselmann (1962) and others. They calculated the spectral energy of bound waves and nonlinear energy transfer among component waves through resonant interactions. Further studies on wind wave dynamics along the lines of the above spectral approach have been intensively made, and it has been suggested that nonlinear energy transfer plays a dominant role in the growth of wind waves (Hasselman *et al.*, 1973), and that bound waves are dominant at higher frequencies (Masuda *et al.*, 1979; Mitsuyasu *et al.*, 1979).

Recently, however, several new characteristics of wind waves have been found, and some authors have attempted to develop nonspectral models in which the effects of nonlinearity dominates. After the finding that the phase velocity of spectral components does not follow the linear water wave theory (Yefimov *et al.*, 1972; Ramamonjiarisoa, 1974), Lake and Yuen (1978) proposed a model based on the dynamics of a coherent nonlinear water wave. In this model, the spectral components other than a single carrier wave are regarded to be non-dispersive bound waves of the carrier wave. After the finding of a strongly vortical region at individual wave crests (Toba *et al.*, 1975; Okuda *et al.*, 1977; Okuda, 1982), Toba (1978) considered that the wind wave is strongly nonlinear phenomenon coupled with the wind induced rotational flow.

As to the higher frequencies, say $f>1.5f_p$ where f_p is a spectral peak frequency, it has been confirmed by various approaches that spectral component waves are bound waves correlated with energy containing components. On the other hand, in regard to the energy containing components, several distinct view points have been proposed as outlined above: linear waves (spectral approach), nonlinear coherent

* Received 22 December 1982; in revised form 29 June 1983; accepted 6 September 1983.

† Geophysical Institute, Faculty of Science, Tohoku University, Sendai 980, Japan.
Present address: Maizuru Marine Observatory, Shimofukui, Maizuru 624, Japan.

waves (Lake and Yuen, 1978) and strongly nonlinear waves coupled with the wind induced rotational flow (Toba, 1978; Tokuda and Toba, 1982). In this paper, I examine the nonlinearity at energy containing frequencies of wind waves in a wind-wave tunnel by measuring the probability density distribution of surface elevation.

If the wind wave is made up of a sum of an infinite number of component waves with random phases, the surface elevation probability distribution satisfies the Gaussian distribution under the central limit theorem. For a stationary process, a deviation of the measured distribution from the Gaussian implies that the component waves are not independent of each other but have non-random character of phase and amplitude, as shown briefly in Appendix A. Because nonlinear wave-wave interaction is the most probable cause of interrelations among components, the measured distribution is discussed under the assumption that the deviation from the Gaussian gives a measure of the nonlinearity of wind waves.

It is well known that the surface elevation distribution is asymmetric due to the existence of bound waves, or second harmonics, of the energy containing components. This was first shown by Kinsmann (1960) in field observations and recently by Huang and Long (1980) in laboratory measurements. Using the weak interaction theory in a random wave field, Phillips (1961) and Longuet-Higgins (1963) showed that the skewness of the surface elevation distribution is proportional to the wave slope and also depends on the spectral form. The dependence of the skewness on the wave slope was confirmed recently by Huang and Long (1980).

On the other hand, the reason for the occurrence of a symmetrical deviation measured by the kurtosis has not yet been clarified. Huang and Long (1980) reported a large negative kurtosis which is independent of the wave slope. According to Tayfun (1980), the contribution of the bound waves to the kurtosis is positive and nearly proportional to the square of the wave slope. The negative kurtosis measured by Huang and Long (1980) contradicts this prediction in sign and in its dependency on the wave slope, so that the measured negative kurtosis is not caused by bound waves of higher frequencies. This fact suggests that the negative kurtosis is associated with the energy containing component waves. To confirm this idea, an artificial time series of the dominant waves was made by excluding the higher harmonic components from the raw wave records by using a band-pass filter, and the surface elevation distribution of the dominant wave was compared with the Gaussian distribution. One of the main purposes of this paper is to determine whether the energy containing component waves are linear waves or nonlinear correlated waves.

In order to conclusively prove the conclusions of this paper, it is necessary to examine the higher order spectra, such as bi- and tri-spectra. However, it requires tedious work to calculate and illustrate the higher order spectra. In the present analyses, therefore, surface elevation distribution is used because of its simplicity.

2. Experiments and data analyses

2.1. Experiments

Experiments were conducted in a wind-wave tunnel 20 m in length, 0.6 m in width and 1.2 m in height, with a constant water depth of 0.6 m, as illustrated in Fig. 1. The surface elevation η was measured with capacitance type wave gauges located at six stations, F=1.85, 3.85, 5.85, 7.85, 10.90 and 13.85 m, where F is the fetch. The amplitude response of the wave gauge is approximately unity up to 8 Hz and reduces to 0.9 at 10 Hz, and the phase

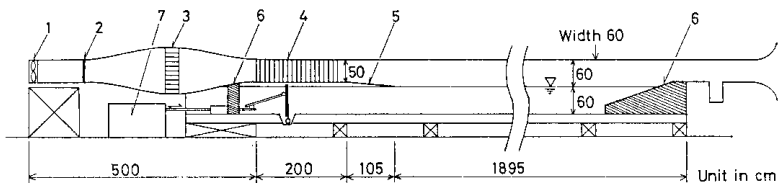

Fig. 1. Schematic picture of the wind-wave tunnel. 1, blower; 2, fine mesh screens; 3, honey comb; 4, coarse mesh grids; 5, transition plate; 6, permeable wave absorber; 7, wave generator.

lag of the wave gauge output is less than 10 degrees up to 8 Hz. Three wind conditions, $U=5.0$, 7.5 and 10.0 m sec^{-1}, were used, where U is the wind speed at the center of the air inlet. The friction velocities estimated from vertical wind profiles by a Pitot-static tube at $F=7$ m were 27.2, 45.9 and 63.5 cm sec^{-1}, respectively.

Power spectra were calculated by the Fast Fourier Transform (FFT) technique, using 2,048 digital data sampled every 0.02 sec and averaging 80 individual raw spectra. The degrees of freedom are 160 and the resolution of frequency is 0.024 Hz. From the spectral peak frequency, f_p, the wave number of the spectral peak k_p was estimated by using the linear dispersion relation. The wave number k_p was used to calculate the representative wave slope $k_p\sqrt{\overline{\eta^2}}$, where $\sqrt{\overline{\eta^2}}$ is the r.m.s. amplitude.

According to recent studies by Ramamonjiarisoa (1974), Lake and Yuen (1978), Tokuda and Toba (1982) and others, the phase velocity of wind waves is slightly larger than that predicted by the linear water wave theory. Therefore, the wave slope calculated by using the linear dispersion relation does not correspond exactly to a real wave slope. The values of the representative wave slope must be slightly larger than the real ones. However, the difference does not greatly affect the results of the present study.

2.2. *Probability density distribution of surface elevation*

The probability density distribution function of surface elevation, $p(\eta)$, and its normalized form, $P(\zeta)\,(=\sqrt{\overline{\eta^2}}p(\eta))$, were calculated from 163,840 digital data sampled every 0.02 sec (length of data is 54.6 min), where $\zeta=\eta/\sqrt{\overline{\eta^2}}$. The $p(\eta)$ was defined as the probability of finding a digital data point between $\eta-\frac{1}{2}\Delta\eta$ and $\eta+\frac{1}{2}\Delta\eta$, where the increment of surface elevation $\Delta\eta$ is selected to be $\sqrt{\overline{\eta^2}}/10$.

In the present study, we examine the third and fourth order cumulants which give measures of the deviations of a distribution from the Gaussian distribution, *i.e.*, the skewness

$$K_3=\frac{1}{(\overline{\eta^2})^{3/2}}\int_{-\infty}^{\infty}\eta^3 p(\eta)\,d\eta \qquad (1)$$

and the kurtosis

$$K_4=\frac{1}{(\overline{\eta^2})^2}\int_{-\infty}^{\infty}\eta^4 p(\eta)d\eta-3\,. \qquad (2)$$

The skewness K_3 gives a measure of asymmetry of a distribution, while the kurtosis K_4 gives a measure of the peakedness of a distribution. For a Gaussian distribution, $K_3=0$ and $K_4=0$. As shown in appendix A, non-zero skewness and kurtosis indicate that the component waves are not independent each other but have a definite phase and amplitude relation among the components. The skewness corresponds to the interaction among a triad of component waves, and the kurtosis to the interaction among a tetrad of component waves.

The waveheight distribution of zero-up-crossing individual waves is also examined to supplement the results of the surface elevation distribution. The waveheight of an individual wave was defined by the average height of the crest relative to the forward and backward trough, as illustrated in Hatori and Toba (1983).

2.3. *Calculation of the dominant waves*

In order to examine the nonlinearity at the energy containing frequencies, an artificial time series is made composed of only spectral component waves at energy containing frequencies, and it is calculated in the following manner.

(i) Digital data are divided into 80 sub-samples, each of which contains 2,048 data points and is 40.96 sec long.

(ii) Complex Fourier coefficients are calculated by the FFT for each sub-samples.

(iii) Fourier coefficients for the frequencies out of range, $f_p-\delta f<f<f_p+\delta f$, are assigned the value of zero.

(iv) These modified Fourier coefficients are inversely transformed by the FFT and a time series composed of the energy containing components are obtained for each sub-sample.

Hereafter, the calculated time series are called the dominant waves, and the skewness and the kurtosis of the surface elevation distribution of the dominant waves are designated as K_3' and K_4', respectively.

The frequency band width δf is selected in order to meet the requirement that the effects of the second harmonics be excluded but most of the energy be retained in the range $f_p-\delta f<f<f_p+\delta f$. Figure 2 shows (a) the normalized power spectrum and (b) the relation of K_3' and

K_4' to a normalized frequency band width under the condition of $U=10.0$ m sec^{-1} and $F=13.85$ m. The values of K_3' and K_4' are almost totally unaffected by the selection of the band width $\delta f/f_p$ in the range $0.3<\delta f/f_p<0.7$. When $\delta f/f_p$ is greater than 0.7, the energy of the harmonic hump in the spectrum is included in the calculation of the dominant waves, and the values of K_3' is affected by the second harmonics. As a result, K_3' is not zero. When $\delta f/f_p$ is less than 0.3, a large amount of the total energy is excluded. From these results, we set the value of δf at $0.5f_p$. The energy contained in this frequency range is 93 to 98 % of the total energy.

A time series of the dominant waves under the same conditions as in Fig. 2 is shown by a dotted line in Fig. 3. The effects of the second harmonics on the wave forms, sharp crests and rounded troughs, disappear from the wave forms of the dominant waves. As seen in the small waves, high frequency ripples also disappear from the records of the dominant waves.

2.4. *Simulation of random waves*

In addition to the non-random character of the phases among component waves, the limitation of the number of component waves and of the data points also produces deviations of the surface elevation distribution from Gaussian. To examine whether these statistical errors have an influence on the surface elevation distribution of the dominant waves, a numerical simulation of random waves was made whose power spectrum is equal to that of the dominant waves shown by the shaded area in Fig. 2a. The random waves are evaluated by the same method as that used for the dominant waves, (i) to (iv)

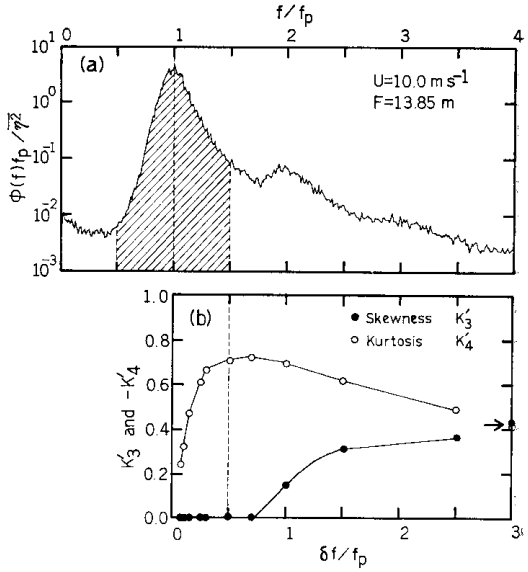

Fig. 2. Normalized power spectrum (a) and relation of skewness K_3' and kurtosis K_4' to the frequency band width of the filter $\delta f/f_p$ (b). The values of K_3' and K_4' indicated by the arrows are for the distribution of the raw wave records. The shaded area in (a) and the broken line in (b) represent the band width employed, $\delta f/f_p=0.5$.

in section 2.3, except that the random phases distributed uniformly over $(0, 2\pi)$ are given to each Fourier component between steps (iii) and (iv). The number of Fourier components and of data points are equal to those of the dominant waves in Figs. 2 and 3.

Figure 4 shows the surface elevation distribution of the simulated random waves. The Gaussian distribution is satisfied fairly well.

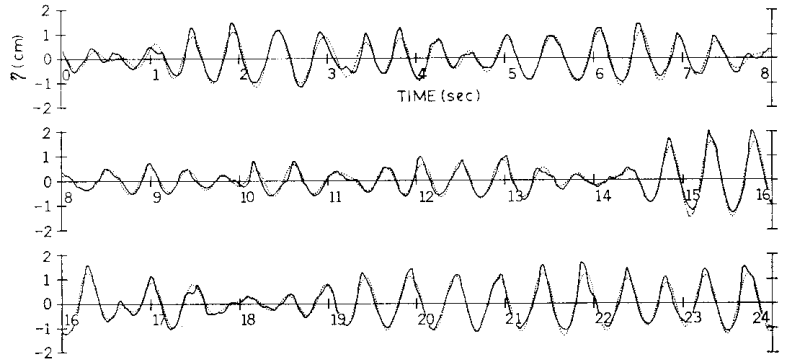

Fig. 3. Raw wave records (solid line) and wave records of the dominant waves (dotted line) under the conditions of $U=10.0$ m sec^{-1} and $F=13.85$ m.

Therefore, if we find the surface elevation distribution of the dominant waves to be non-Gaussian, it can be said that the deviation from Gaussian is not due to statistical errors but rather due to the non-random character of the phase and amplitude of the energy containing components.

3. Results and discussion

3.1. Surface elevation distribution of raw wave records

A typical surface elevation distribution of the raw wave records is shown in Fig. 5, where $U=10.0$ m sec^{-1} and $F=13.85$ m. Open circles are for the experimental results and the solid line shows the Gaussian distribution. The distribution is highly non-Gaussian and has a positive skewness, $K_3=0.462$, and a negative kurtosis, $K_4=-0.409$. The values of K_3 and K_4 for all the runs are summarized in Table 1. Every distribution has a positive skewness and a negative kurtosis.

The positive skewness is clearly due to the

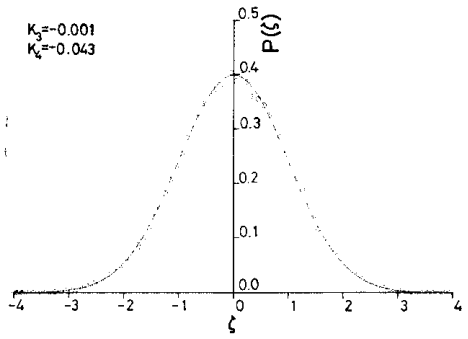

Fig. 4. Normalized surface elevation distribution of simulated random waves. The solid line shows the Gaussian distribution.

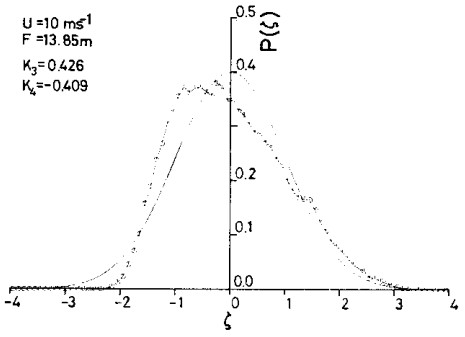

Fig. 5. Normalized surface elevation distribution of the raw wave records under the conditions of $U=10.0$ m sec^{-1} and $F=13.85$ m. The solid line shows the Gaussian distribution.

Table 1. Statistical characteristics of wind waves. f_p, spectral peak frequency; $\sqrt{\overline{\eta^2}}$, root-mean-square amplitude; $\Delta f/f_p$, normalized 1/10 holding spectral band width; $k_p\sqrt{\overline{\eta^2}}$, representative wave slope; K_3, skewness; K_4, kurtosis; K_3', skewness of dominant waves and K_4' kurtosis of dominant waves.

u_* cm sec^{-1}	Fetch m	f_p Hz	$\Delta f/f_p$	$\sqrt{\overline{\eta^2}}$ cm	$k_p\sqrt{\overline{\eta^2}}$	K_3	K_4	K_3'	K_4'
63.85	1.85	4.61	0.635	0.27	0.233	0.297	−0.633	0.001	−0.645
	3.85	3.47	0.542	0.47	0.227	0.347	−0.506	0.001	−0.643
	5.85	2.93	0.533	0.62	0.215	0.418	−0.442	0.002	−0.652
	7.85	2.66	0.468	0.81	0.231	0.425	−0.412	0.001	−0.656
	10.90	2.25	0.456	1.01	0.205	0.401	−0.440	−0.001	−0.691
	13.85	2.05	0.440	1.24	0.210	0.426	−0.409	0.001	−0.705
45.9	1.85	6.27	0.603	0.12	0.196	0.149	−0.737	−0.004	−0.629
	3.85	4.47	0.508	0.27	0.214	0.324	−0.588	0.000	−0.707
	5.85	3.81	0.474	0.40	0.235	0.417	−0.451	0.000	−0.700
	7.85	3.20	0.443	0.53	0.219	0.392	−0.505	0.001	−0.708
	10.90	2.69	0.409	0.67	0.194	0.353	−0.530	0.000	−0.739
	13.85	2.44	0.430	0.79	0.190	0.375	−0.479	0.001	−0.715
27.2	1.85	——	——	——	——	——	——	——	——
	3.85	6.18	0.577	0.09	0.146	0.217	−0.549	−0.000	−0.516
	5.85	5.25	0.456	0.16	0.173	0.213	−0.605	0.000	−0.612
	7.85	4.47	0.443	0.23	0.188	0.340	−0.554	−0.000	−0.655
	10.90	3.59	0.456	0.31	0.163	0.378	−0.453	0.000	−0.625
	13.85	3.27	0.440	0.42	0.180	0.342	−0.458	−0.000	−0.661

second harmonics of the energy containing components, and this was confirmed in the previous section by the fact that the exclusion of the energy hump at $2f_p$ in the spectrum leads to a decrease in the skewness (see Fig. 2). According to the weak interaction theory in a random wave field, K_3 is proportional to the wave slope and depends on the spectral form (Phillips, 1961; Longuet-Higgins, 1963), and is approximately given by

$$K_3 \simeq 3\, k_p \sqrt{\overline{\eta^2}} \qquad (3)$$

for a narrow band spectrum (Tayfun, 1980). In Fig. 6, K_3 is plotted against $k_p\sqrt{\overline{\eta^2}}$, together with (3) and an empirical relation $K_3 = 4\, k_p \sqrt{\overline{\eta^2}}$ derived by Huang and Long (1980). The skewness of the present experiment shows a weak dependence on $k_p\sqrt{\overline{\eta^2}}$ except at short fetches (surrounded by circles in the figure), and the values are smaller than those predicted by Eq. (3) and by the Huang and Long relation.

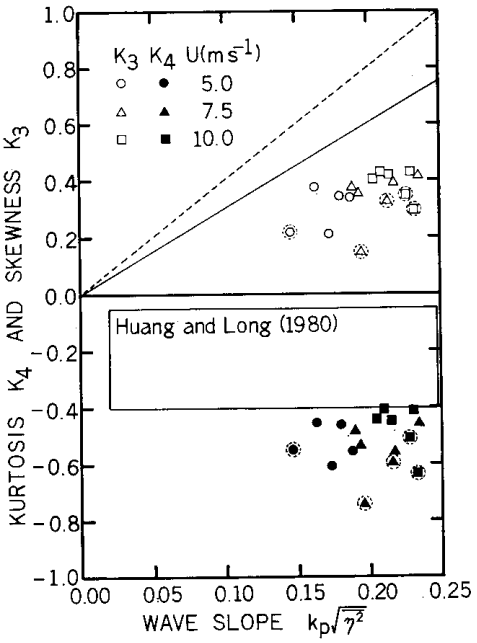

Fig. 6. Measured skewness K_3 and kurtosis K_4 plotted against the wave slope $k_p\sqrt{\overline{\eta^2}}$. Solid and dashed lines show Eq. (3) and an empirical relation by Huang and Long (1980), respectively. The rectangle shows the range of K_4 observed by Huang and Long (1980). The data surrounded by dashed circles indicate those at the first and second fetches.

The values of K_3 at the first or second value of fetch are smaller than the nearly constant values at larger fetches when the wind condition is fixed. Since the wave slope $k_p\sqrt{\overline{\eta^2}}$ under a fixed wind condition does not vary so much, this tendency may be due to the fact that the normalized spectral band width, $\Delta f/f_p$ in Table 1, at short fetches is larger than those at larger fetches, where Δf is the 1/10 holding spectral band width.

Next, we examine the kurtosis K_4. Figure 6 shows K_4 as a function of $k_p\sqrt{\overline{\eta^2}}$. These results also agree with those of Huang and Long (1980), though the magnitude of K_4 in the present experiment is larger than in their results. According to Tayfun (1980), the contribution of bound waves to the kurtosis in a narrow band random wave field is approximately given by

$$K_4 \simeq 12(k_p\sqrt{\overline{\eta^2}})^2 . \qquad (4)$$

The present results contradict Tayfun's prediction in sign and in dependency on the wave slope. Thus the bound waves cannot account for the measured negative kurtosis.

Another interesting feature is that the absolute values of K_4 increase with decrease of K_3 as shown in Fig. 7, where the results of Huang and Long (1980) are also included. This relation between K_3 and K_4 differs from Tayfun's prediction,

$$K_4 = \frac{4}{3} K_3^2 \qquad (5)$$

derived from Eqs. (3) and (4).

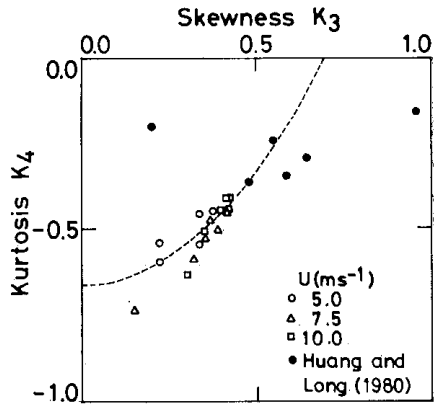

Fig. 7. Relation between skewness K_3 and kurtosis K_4. The broken curve represents Eq. (6) with $K_4' = -0.66$.

In the present experiment, we obtained values of K_3 and K_4 which differ in magnitude from the results of a similar laboratory experiment by Huang and Long (1980). The reason for the differences is not clear at present, but may be due to a difference in experimental conditions. The data of Huang and Long (1980) were measured only at a fixed fetch and partly include data under extremely high and low wind speed.

3.2. Surface elevation distribution of the dominant waves

Figure 8 shows the surface elevation distribution of the dominant waves under the conditions $U=10.0$ m sec^{-1} and $F=13.85$ m. The distribution is almost symmetrical, and the skewness is very small and $K_3'=0.001$. This is clearly due to the exclusion of second harmonics. However, the distribution remains highly non-Gaussian. The distribution is concentrated in the range $|\zeta|<3.0$, the probability density is smaller than the Gaussian in the ranges $|\zeta|<1.0$ and $|\zeta|>2.0$ and it is larger than the Gaussian in the range $1.0<|\zeta|<2.0$. The kurtosis is negative and $K_4'=-0.705$.

Figure 9 shows the surface elevation distribution of the dominant waves for all the runs, and the skewness K_3' and kurtosis K_4' are listed in Table 1. The distributions are almost independent of the wind speed and the fetch, though the surface elevation distribution of the raw wave records depends on them. The mean value of skewness is $\bar{K}_3'=0.000\pm0.011$ and the mean value of kurtosis is $\bar{K}_4'=-0.662\pm0.051$. The magnitude of K_4' is greater than the skewness K_3 and the kurtosis K_4 for the raw wave records.

From the above results, it is concluded that the energy containing components have non-random character of phase and amplitude among the components, and this produces a negative kurtosis. Thus, the random phase approximation is not valid and nonlinear processes occur in the energy containing frequency range. As shown in appendix A, non-zero kurtosis implies the existence of the nonlinear interaction among a tetrad of component waves.

According to the weak interaction theory, wave-wave interaction among a tetrad of components generally involves weakly time dependent components, owing to resonant interaction, so that a definite value of the kurtosis cannot be obtained; the kurtosis weakly depends on time. By applying the weak interaction theory to a random wave field, Longuet-Higgins (1963) predicted that the kurtosis K_4 would be of the same order as $(k_p\sqrt{\bar{\eta}^2})^2$, or K_3^2. The measured kurtosis of the dominant waves K_4', however, is of the same order as the skewness K_3 and one order of magnitude greater than the above prediction. In any case, the theory, which assumes the random phases among components, does not account for the magnitude of measured K_4'.

3.3. Relation between K_4 and K_4'

As shown in section 3.2, the kurtosis of the dominant waves K_4' is almost constant, and its magnitude is greater than that for the raw wave records K_4. The difference between K_4' and K_4 may be explained by introduce of the contribution of bound waves. The contribution of the second order bound waves to K_4 is given by Eq. (4) for a narrow band random

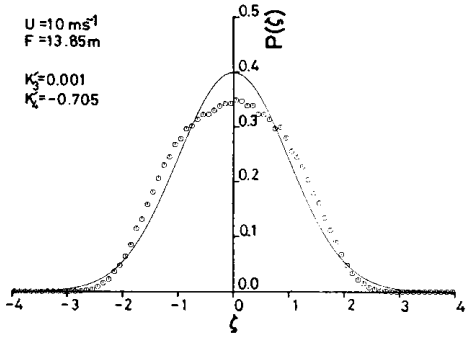

Fig. 8. Normalized surface elevation distribution of the dominant waves under the same conditions as in Figs. 3 and 5. The solid line shows the Gaussian distribution.

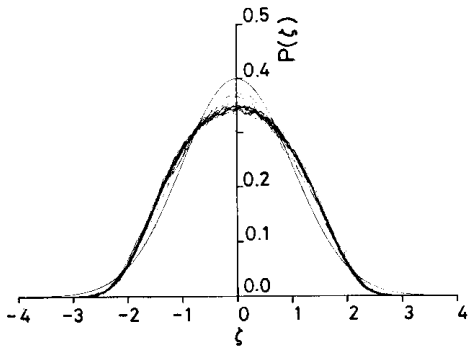

Fig. 9. Normalized surface elevation distributions of the dominant waves for all the runs.

wave field. Power spectra of the present study are, however, rather broad and the dominant wave is not a random wave field, so that we cannot employ Eq. (4) directly. Let us assume that the kurtosis expressed by the skewness Eq. (5) is also valid for the present situation, because the skewness seems to reflect the effects of the bound waves rather than the wave slope in the present experiment. Then, the kurtosis for the raw wave records is approximately expressed by a sum of the contributions of the energy containing frequencies, K_4', and of the second harmonics Eq. (5),

$$K_4 = K_4' + \frac{4}{3}K_3^2 . \qquad (6)$$

The broken line in Fig. 7 is a curve where $K_4' = -0.66$, which was experimentally derived in *3.2*. Equation (6) coincides well with the measured data, except for the two data points measured by Huang and Long (1980). The disagreement of the two points may be caused by the fact that the data were collected under conditions of extremely high and low wind speeds. It is concluded from the above results that the kurtosis of the raw wave records is given by a sum of the contribution of the energy containing components and a minor contribution of the bound waves.

3.4. Waveheight distribution of the dominant waves

Figure 10 shows a normalized waveheight distribution of the dominant waves under the conditions of $U = 10.0$ m sec^{-1} and $F = 13.85$ m (large circles). In the figure, small circles are for the waveheight distribution of the simulated random wave field as described in *2.4*. The Rayleigh distribution derived by Longuet-Higgins (1952) for a narrow band spectrum is also shown by a thin solid line. The waveheight distribution of the simulated random waves is slightly distorted from the Rayleigh distribution because of the finite band width of the simulated spectrum and the use of a different definition of waveheight.

The probability density of the original dominant waves is centered at the mean waveheight and is greater than that of the simulated random waves in the range $0.9\,\bar{H} < H < 1.6\,\bar{H}$, that is, the individual waves are more uniform in size than those for the random Gaussian wave field.

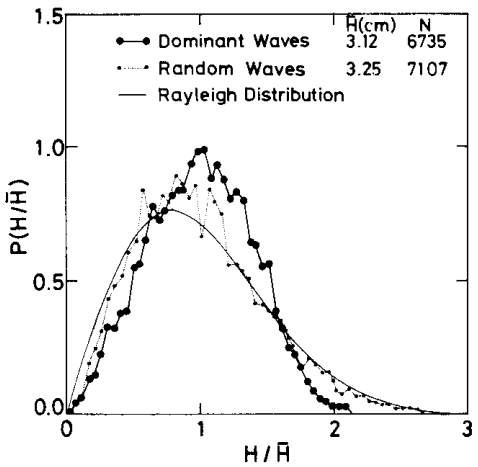

Fig. 10. Normalized waveheight distribution of the dominant waves in comparison with simulated random waves and the Rayleigh distribution for a narrow band spectrum. $\bar{H}$ represents the mean waveheight and N the number of individual waves.

The above features also hold for the waveheight distribution of the raw wave records.

Huang and Long (1981) recently reported a waveheight distribution similar to the present one but the cause of the deviation from the random wave field was not discussed. The present results show that this deviation arises from some nonlinear mechanism in the energy containing frequency range.

Hatori and Toba (1983) investigated the process of transition of regular water waves to wind waves under the action of wind, and found that a regular wavetrain evolves into a strongly modulated wavetrain, and the strongly modulated wavetrain becomes a somewhat stabilized uniform wavetrain consisting of larger waves than the preceding stage after the occurrence of the mutual coalescences of waves at the troughs of modulation. If the mechanism of these nonlinear processes holds for real wind waves, the demodulation by the mutual coalescence of waves can be a cause for the concentration of the waveheight distribution, and this concentration necessarily leads to the deviation of the surface elevation distribution from the Gaussian as found in *3.2*.

Finally let us refer briefly to wave breaking as a possible cause of the non-Gaussian distribution. In the present experiments, wave break-

ing was observed in the case of $U=10.0\ \mathrm{m\ sec^{-1}}$ and $F\geqslant 7$ m. Judging from the similarity of the surface elevation distributions of the dominant waves regardless of the existence or absence of wave breaking, we can conclude that the distributions are scarcely affected by wave breaking in the range of the present experimental conditions. Under extremely high wind conditions, however, there is the possibility of wave breaking distorting the distributions. Observations under such conditions were not carried out in this study.

4. Conclusions

The surface elevation distribution of raw wave records and of dominant waves in which the higher harmonic components are excluded were examined in a wind-wave tunnel, and led to the following conclusions. (1) The positive skewness of the measured distributions is due to the higher harmonic components of the energy containing components, as already shown by many authors. (2) The negative kurtosis of the measured distributions is mainly due to some nonlinearity of the dominant waves themselves, or to nonlinear interaction among a tetrad of energy containing components.

The non-Gaussian nature of the dominant waves found in this paper shows that the component waves at energy containing frequencies cannot be considered as linear free waves. This fact indicates that the spectral model cannot be applied to wind waves, or, at least, must be modified considerably, since the spectral model assumes that the wind waves are expressed by the sum of linear free waves to a first order approximation, or that the component waves in the energy containing frequency range are composed of linear free waves. The wind waves must be modelled by using a new and more appropriate approach which attaches weight to the nonlinearity at energy containing frequencies, such as in the model of Lake and Yuen (1978).

Acknowledgements

The author would like to thank Prof. Y. Toba, the late Dr. S. Kawai, Dr. K. Okuda and Mr. H. Kawamura of the Physical Oceanography Laboratory of Tohoku University for their valuable discussion and comments throughout the course of this study. The author is also grateful to the reviewers for valuable comments on this paper. This study was partially supported by a Grant-in-Aid for Scientific Research by the Ministry of Education, Science and Culture, Project No. 56116006.

References

Hasselmann, K. (1962): On the non-linear energy transfer in a gravity wave spectrum. Part 1. J. Fluid Mech., **12**, 481–500.

Hasselmann, K., T.B. Barnett, E. Bouws, H. Carlson, D.E. Cartwrite, K. Enke, J.A. Ewing, H. Gienapp, D.E. Hasselmann, P. Kruseman, A. Meerburg, P. Müller, D.J. Olber, K. Richter and W. Sell (1973): Measurements of wind-wave growth and swell decay during the Joint North Sea Wave Project (JONSWAP), Deut. Hydrogr. Z., Suppl. A, 8, No. 12.

Hatori, M. and Y. Toba (1983): Transition of mechanically generated regular waves to wind waves under the action of wind. J. Fluid Mech., **130**, 397–409.

Huang, N.E. and S.R. Long (1980): An experimental study of the surface elevation probability distribution and statics of wind-generated waves. J. Fluid Mech., **101**, 179–200.

Huang, N. E. and S. R. Long (1981): An experimental study of the statistical properties of the wind generated gravity waves. IUCRM Symposium on Wave Dynamics and Radio Probing of the Ocean Surface, May 13–20, 1981, Miami Beach.

Kinsman, B. (1960): Surface waves at short fetches and low wind speed—a field study. Chesapeake Bay Inst., Johns Hopkins Univ. Tech. Rep. No. 19.

Lake, B.M. and H.C. Yuen (1978): A new model for nonlinear wind waves. Part 1. Physical model and experimental evidence. J. Fluid Mech., **88**, 33–62.

Longuet-Higgins, M. S. (1952): On the statistical distribution of the heights of sea waves. J. Mar. Res., **11**, 245–266.

Longuet-Higgins, M.S. (1963): The effect of nonlinearities on statistical distributions in the theory of sea waves. J. Fluid Mech., **17**, 459–480.

Masuda, A., Y.Y. Kuo and H. Mitsuyasu (1979): On the dispersion relation of random gravity waves. Part 1. Theoretical framework. J. Fluid Mech., **92**, 717–730.

Mitsuyasu, H., Y.Y. Kuo and A. Masuda (1979): On the dispersion relation of random gravity waves. Part 2. An experiment. J. Fluid Mech., **92**, 731–749.

Okuda, K. (1982): Internal flow structure of short wind waves. Part 1. On the internal vorticity

structure. J. Oceanogr. Soc. Japan, **38**, 28-42.
Okuda, K., S. Kawai and Y. Toba (1977): Measurement of skin friction distribution along the surface of wind waves. J. Oceanogr. Soc. Japan, **33**, 190-198.
Phillips, O.M. (1960): On the dynamics of unsteady gravity waves of finite amplitude. Part 1. J. Fluid Mech., **9**, 193-217.
Phillips, O.M. (1961): On the dynamics of unsteady gravity waves of finite amplitude. Part 2. J. Fluid Mech., **11**, 143-155.
Ramamonjiarisoa, A. (1974): Contribution a l'étude de la structure statistique et des mécanismes de génération des vagues de vent. Thesis, Université de Provence.
Tayfun, M.A. (1980): Narrow-band nonlinear sea waves. J. Geophys. Res., **85**, 1548-1552.
Tick, L.J. (1959): A non-linear random model of gravity waves. Part I. J. Math. Mech., **8**, 643-652.
Toba, Y. (1978): Stochastic form of the growth of wind waves in a single parameter representation with physical implication. J. Phys. Oceanogr., **8**, 494-507.
Toba, Y., M. Tokuda, K. Okuda and S. Kawai (1975): Forced convection accompanying wind waves. J. Oceanogr. Soc. Japan, **31**, 192-198.
Tokuda, M. and Y. Toba (1982): Statistical characteristics of individual waves in laboratory wind waves. I. Individual wave spectra and similarity structure. J. Oceanogr. Soc. Japan, **37**, 243-258.
Yefimov, V.V., Yu. P. Solov'yev and G.N. Khristoforov (1972): Observational determination of the phase velocities of spectral components of wind waves. Izv., Atmos. Ocean. Phys., **8**, 246-251.

Appendix A

Relation of skewness and kurtosis to the interaction among component waves

When the surface elevation $\eta(t)$ is a stationary process and can be represented by a Fourier Stiertjes integral

$$\eta(t)=\int_{-\infty}^{\infty} \mathrm{d}Z(\omega)e^{i\omega t}\,, \qquad \text{(A-1)}$$

the skewness is given by

$$K_3=\frac{1}{\langle\eta^2\rangle^{3/2}} \iint_{\omega_1+\omega_2+\omega_3=0}^{\infty} \langle \mathrm{d}Z(\omega_1)\mathrm{d}Z(\omega_2)\mathrm{d}Z(\omega_3)\rangle\,, \qquad \text{(A-2)}$$

where $\langle\ \rangle$ is the ensemble average and $\langle\eta(t)\rangle=0$. For the Gaussian process, $K_3=0$, because the components are independent of each other. When a triad of component waves, satisfying $\omega_1+\omega_2+\omega_3=0$, has a definite phase and amplitude relation independent of ensembles, they contribute to the non-zero skewness. The most probable cause for a definite phase and amplitude is the nonlinear interaction among a triad of component waves. A well known example is the second harmonics.

In the same way as the skewness, the kurtosis is represented by

$$K_4=\frac{1}{\langle\eta^2\rangle^2} \iiint_{\omega_1+\omega_2+\omega_3+\omega_4=0}^{\infty} \langle \mathrm{d}Z(\omega_1)\mathrm{d}Z(\omega_2)\mathrm{d}Z(\omega_3) \times \mathrm{d}Z(\omega_4)\rangle -3=\frac{1}{\langle\eta^2\rangle^2} \times \iiint_{\substack{\omega_1+\omega_2+\omega_3+\omega_4=0 \text{ and} \\ \omega_1+\omega_2\neq 0,\ \omega_1+\omega_3\neq 0 \\ \text{and } \omega_2+\omega_3\neq 0}}^{\infty} \langle \mathrm{d}Z(\omega_1)\mathrm{d}Z(\omega_2)\mathrm{d}Z(\omega_3)\mathrm{d}Z(\omega_4)\rangle\,. \qquad \text{(A-3)}$$

The contribution from the power spectrum on the planes, $\omega_1+\omega_2=0$, $\omega_1+\omega_3=0$ and $\omega_2+\omega_3=0$, is excluded from the integral by a factor of 3. When a tetrad of component waves, satisfying $\omega_1+\omega_2+\omega_3+\omega_4=0$ and $\omega_1+\omega_2\neq 0$, $\omega_1+\omega_3\neq 0$ and $\omega_2+\omega_3\neq 0$, has a definite phase and amplitude relation, they contribute to the non-zero kurtosis. The most probable cause for a definite phase and amplitude relation among the components is the nonlinear interactions among a tetrad of component waves. One example of this is the third harmonics.

Appendix B

Relation between the waveheight and surface elevation distributions of the dominant waves

The probability density of the waveheight distribution shown in Fig. 10 is centered at the mean waveheight and is limited in the range $H\leqslant 2.1\overline{H}$, and is greater than that of the simulated random waves in the range $0.9\,\overline{H}<H<1.6\,\overline{H}$. This inequality is converted into $2.2\sqrt{\overline{\eta^2}}<H<4.0\sqrt{\overline{\eta^2}}$, where we use an empirical relation derived from the present data $\overline{H}=2.5\sqrt{\overline{\eta^2}}$. Since the contribution of individual wave forms to the surface elevation probability density is large at peaks and troughs, it is inferred from the above inequality that the surface elevation distribution probability density is larger than the Gaussian distribution in the range $1.1<|\zeta|<2.0$. This range agrees with the range of excess values found in section *3.2*.

主要周波数帯における実験室の風波の非線形性
1. 水位の確率密度分布

羽 鳥 光 彦*

要旨: 水位の確率密度分布の測定により，風洞水槽における風波の非線形性について調べた．生の記録の水位分布は正のスキューネス（$K_3=0.21\sim0.43$）と負のクルトシス（$K_4=-0.74\sim-0.41$）を持ち，その大きさはフェッチと風速に依存した．スキューネスの値は，高調波の影響を考慮に入れたランダムな波の場における弱非線形理論（Tayfun, 1980）の予測と定性的に一致した．しかし，クルトシスはその符号自体が予測と違っていた．

エネルギーを含む成分の非線形性を調べるため，高調波を一種のバンドパスフィルターを用いて除去した．フィルターされた波の水位分布は，スキューネスの著しい減少（$\overline{K_3}'=0$）を示したが，依然として非ガウス的な特徴を示した．クルトシスはフェッチと風速に依らない大きな負の値（$\overline{K_4}'=-0.66$）であった．これらの結果より，負のクルトシスはエネルギーを含む成分間の位相と振幅がランダムでないために生じたものであり，主要周波数帯において非線形相互作用が起っていると結論される．

* 東北大学理学部地球物理学科
〒980 宮城県仙台市荒巻字青葉
現所属：舞鶴海洋気象台
〒624 京都府舞鶴市下福井大野辺 901